Sensors and Materials, Vol. 37, No. 2 (2025) 557–562
MYU Tokyo

S & M 3933

Vacuum UV- and Radiation-induced Luminescence Properties of $Sr_3Y(PO_4)_3$ Synthesized by Optical Floating Zone Technique

Kai Okazaki,[1*] Masanori Koshimizu,[2] Daisuke Nakauchi,[1]
Yuma Takebuchi,[3] Kensei Ichiba,[1] Haruaki Ezawa,[1]
Takumi Kato,[1] Noriaki Kawaguchi,[1] and Takayuki Yanagida[1]

[1]Nara Institute of Science and Technology (NAIST), 8916-5 Takayama-cho, Ikoma, Nara 630-0192, Japan
[2]Shizuoka University, 3-5-1 Johoku, Naka-ku, Hamamatsu City, Shizuoka 432-8011, Japan
[3]Utsunomiya University, 7-1-2 Yoto, Utsunomiya, Tochigi 321-8585, Japan

(Received October 31, 2024; accepted December 16, 2024)

Keywords: phosphate single crystal, photoluminescence, scintillation, radiation detection

A $Sr_3Y(PO_4)_3$ single crystal was grown by the optical floating zone technique using four xenon arc lamps. The photoluminescence and scintillation properties in the vacuum ultraviolet (VUV)–visible range were investigated. A broad emission peak appeared at 300–600 nm under the irradiation of both VUV light and X-rays. The scintillation decay time constants were obtained to be 40 and 370 ms. They would be respectively related to self-trapped excitons and some defects. The light yield and energy resolution of $Sr_3Y(PO_4)_3$ were revealed to be 260 photons/5.5 MeV-α and 19%, respectively, by measuring pulse height spectra of ^{241}Am α-rays (5.5 MeV).

1. Introduction

Phosphors for ionizing radiation detection are categorized into scintillators and storage-type phosphors.[1–3] Scintillators immediately convert ionizing radiation into low-energy photons after absorbing the incident high-energy radiation.[4] In the case of storage-type phosphors, they capture carriers that are generated by incident radiation at trapping centers and emit photons upon stimulation by external energy sources such as heat and light.[5] The fluorescence phenomena induced by external heat and light are recognized as thermoluminescence (TL) and optically stimulated luminescence (OSL), respectively.[6] The application fields of the above phosphors are widespread: medical,[7,8] security,[9] and personal dose monitoring.[10,11] The required properties for the materials vary depending on the application; therefore, appropriate materials are selected for use in terms of their physical and chemical properties such as luminescence intensity, decay time, density, effective atomic number (Z_{eff}), and hygroscopicity. Further search of new scintillators and storage-type phosphors has been conducted to improve their performance and satisfy the required standards for radiation detection.[2,12–19]

*Corresponding author: e-mail: okazaki.kai.of0@ms.naist.jp
https://doi.org/10.18494/SAM5427

ISSN 0914-4935
https://myukk.org/

Scintillators for α-ray measurements are especially used in monitoring radioactive contamination and its spatial location.[20–23] Alpha and high beta particle emitters have been detected in the reactor buildings of the Fukushima Daiichi Nuclear Power Station (FDNPS). The scintillators are required to have low–medium Z_{eff} to distinguish the signals between α-rays and noises such as γ-rays. Furthermore, high light yields (*LY*s) and energy resolutions are important for improving the detection efficiencies and discrimination abilities for nuclear species such as in the case of U and Pu isotopes. Ag-doped ZnS has been conventionally mounted and used as α-ray survey meters.[22,24] The Z_{eff} of 27 and the *LY* of 38000 photons/MeV[25] are ideal performance characteristics; however, the energy resolution is in sufficient for distinguishing the energies from different types of α-rays. The material form of ZnS is polycrystal line; therefore, scatterings of scintillation light at some defects and grain boundaries can lead to a decrease in energy resolution.

A $Sr_3Y(PO_4)_3$ single crystal has potential for scintillator use in α-ray measurements because it has a Z_{eff} of 33, which is close to that of ZnS, and has high transparency, which can reduce the scattering of scintillation light. In addition to the above characteristics, phosphates including $A_{3B}(PO_4)_3$-type materials (*A* and *B* are respectively alkaline earth metal elements and rare-earth elements)[26,27] have been reported to show bright luminescence in the visible range, which matches the wavelength sensitivities of conventional Si-based detectors. This is an advantage for detector applications because scintillators are used in combination with photodetectors. In this study, the growth of a $Sr_3Y(PO_4)_3$ single crystal and its luminescence and scintillation properties were investigated.

2. Materials and Methods

A $Sr_3Y(PO_4)_3$ single crystal was grown by the floating zone (FZ) method. $SrCO_3$ (4N), Y_2O_3 (4N), and $NH_4H_2PO_4$ (4N) were used as raw materials. They were weighed in a stoichiometric ratio and mixed to homogeneity with a mortar and pestle. Then, they were transferred into an aluminum crucible and sintered at 1200 ℃ for 12 h for decarbonization. The obtained powders were ground and molded into a rod shape by applying a hydrostatic pressure of 10 MPa. The rod was sintered at 1200 ℃ for 10 h. By using the rod and an FZ furnace having four xenon arc lamps (Crystal Systems, FZ-T-12000-X-VPO-PC-YH), crystal growth was conducted.

The powder X-ray diffraction (XRD) pattern was measured with a diffractometer (Rigaku, MiniFlex600). Vacuum UV (VUV) excitation and VUV-excited emission spectra were measured at the UVSOR synchrotron facility (BL-7B). An X-ray-induced scintillation spectrum, a decay curve, and pulse height spectra of ^{241}Am α-rays (5.5 MeV) and 137Cs γ-rays (0.662 MeV) were measured with our original setups.[9,28]

3. Results and Discussion

Figure 1 shows the photograph and XRD pattern of the prepared $Sr_3Y(PO_4)_3$ sample. The surfaces of the sample were polished for the luminescence and scintillation measurements. The length and thickness were roughly 2–4 mm and 1 mm, respectively. The sample was transparent

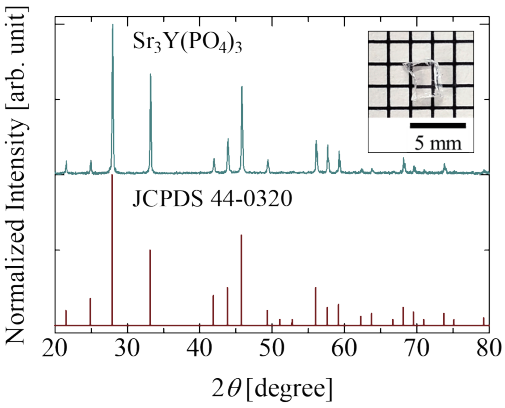

Fig. 1. (Color online) Photograph (inset) and XRD patterns of $Sr_3Y(PO_4)_3$.

and colorless. To confirm the crystalline phase, the XRD pattern was investigated. The pattern matched with a reference from the JCPDS card (44-0320). Furthermore, no other phases such as SrO and Y_2O_3 were observed; hence, the sample had the single phase of $Sr_3Y(PO_4)_3$ with a eulytite-type structure.[29]

Figure 2 shows the VUV excitation and emission spectra of $Sr_3Y(PO_4)_3$. Under excitation light at 170 nm, a broad emission peak appeared at 300–600 nm. Similar emission spectral features were confirmed in $Ba_3Y(PO_4)_3$[26] and some phosphates.[30] From the spectral feature and large Stokes shift, the emission origin is thought to be related to self-trapped excitons (STEs). A photoluminescence (PL) excitation peak at 100–200 nm can be due to band-to-band transitions between $(PO_4)^{3-}$.[31,32] An excitation peak at 200 nm was also observed in other phosphate materials.[26,31] Thus, it can be due to charge transfer transitions between Y^{3+} and O^{2-}. Figure 3 shows the X-ray-induced scintillation spectrum and scintillation decay curve of $Sr_3Y(PO_4)_3$. A broad emission peak was confirmed at 300–600 nm as well as the VUV-excited emission spectrum (Fig. 2). A scintillation decay curve was measured by monitoring at 160–650 nm. The decay curve was fitted by a sum of three exponential functions. The fastest component was due to an instrumental response function (IRF) that was caused by an excitation source. In a previous report of an X-ray-induced scintillation spectrum of $Ba_3La(PO_4)_3$, the spectrum convoluted the two origins: STEs and some defects.[27] Hence, it was reasonable that two decay components due to the material appeared. The second component had a decay time constant of 40 ms. The order of the decay time constant matched the value of triplet–singlet transitions of STEs confirmed in $ScPO_4$ (10 ms);[30] thus, the component was considered to be related to STEs. The slowest component had a decay time constant of 370 ms. The origin is unclear; however, it could be associated with defects according to the scintillation spectra due to STEs.

Figure 4 shows the pulse height spectrum of ^{241}Am α-rays (5.5 MeV) measured using $Sr_3Y(PO_4)_3$. As a reference for estimating the *LY* of $Sr_3Y(PO_4)_3$, the spectrum of ^{137}Cs γ-rays measured using Gd_2SiO_5 (GSO, *LY*: 7500 photons/MeV[33]) is also displayed. $Sr_3Y(PO_4)_3$ shows a clear full energy absorption peak. By comparing the channel number of this peak with that of a photoabsorption peak of GSO, the *LY* of $Sr_3Y(PO_4)_3$ was calculated to be 260 photons/5.5 MeV-α. This value was much lower than that of Ag-doped ZnS. However, the energy resolution

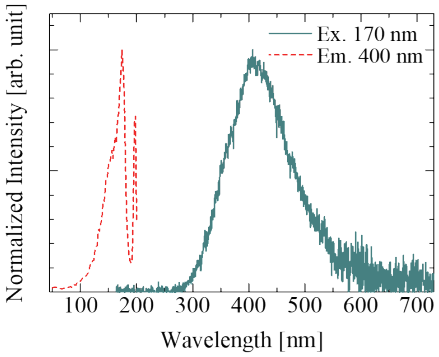

Fig. 2. (Color online) VUV excitation and emission spectra of $Sr_3Y(PO_4)_3$. Solid line shows an emission spectrum under excitation at 170 nm. Dashed line shows an excitation spectrum monitored at 400 nm.

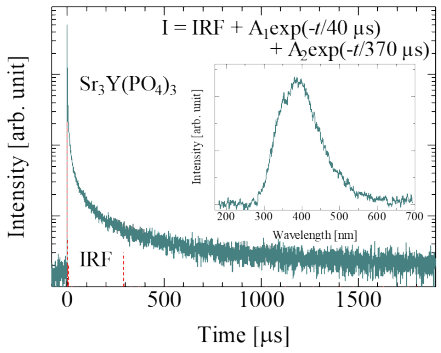

Fig. 3. (Color online) X-ray-induced scintillation spectrum (inset) and decay curve of $Sr_3Y(PO_4)_3$. Dashed line shows IRF.

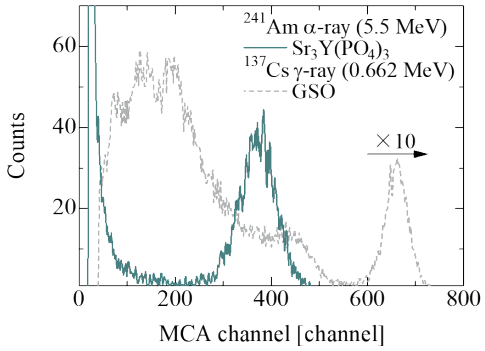

Fig. 4. (Color online) Pulse height spectra of ^{241}Am α-rays measured using $Sr_3Y(PO_4)_3$ and ^{137}Cs γ-rays measured using GSO.

was calculated to be 19% in $Sr_3Y(PO_4)_3$, which was superior to that of Ag-doped ZnS. $Sr_3Y(PO_4)_3$ was reported to show TL when stimulated at 50–150 °C.[34,35] Therefore, some carriers generated by inserting ionizing radiation were captured at the trapping centers, which can be stimulated by the energy at 50–150 °C, and this led to the low *LY*.[36] In some materials, the amount and type of trapping center were successfully changed by doping impurities.[37,38] Furthermore, PL emission efficiencies can also be increased. According to the Robins model, *LY* is proportional to band gap energy, energy transfer efficiency, and PL emission efficiency.[39] Hence, the *LY* of this material could be improved by controlling the traps such as by doping cations of different valences with host compositions [37] or by introducing luminescence centers, which can lead to high emission efficiencies.[29,40,41]

4. Conclusions

A $Sr_3Y(PO_4)_3$ single crystal was synthesized by the FZ method. Its luminescence and scintillation properties were examined. It showed a broad emission peak at 300–600 nm under both VUV light and X-rays. The scintillation decay time constants of 40 and 370 ms were

confirmed. The former could be related to STEs and the latter to some defects. A pulse height spectrum of ^{241}Am α-rays (5.5 MeV) was measured using $Sr_3Y(PO_4)_3$. A clear full energy peak appeared, and the *LY* and energy resolution were respectively calculated to be 260 photons/5.5 MeV-α and 19%. This good energy resolution is advantageous over the conventional scintillator for α-ray measurements, although the material needs a major improvement in *LY*.

Acknowledgments

This work was supported by MEXT Grants-in-Aid for Scientific Research A (22H00309), Scientific Research B (23K21827, 23K25126, and 24K03197), Exploratory Research (22K18997), Early-Career Scientists (23K13689), and JSPS Fellows for Young Scientists (23KJ1592). Suzuki Foundation, Asahi Glass Foundation, and Konica Minolta Science and Technology Foundation are also acknowledged. Part of this work was conducted at the BL7B of UVSOR Synchrotron Facility, Institute for Molecular Science (IMS program 23IMS6026).

References

1 S. E. Derenzo, M. J. Weber, E. Bourret-Courchesne, and M. K. Klintenberg: Nucl. Instrum. Methods Phys. Res., Sect. A **505** (2003) 111.
2 W. W. Moses: Nucl. Instrum. Methods Phys. Res., Sect. A **487** (2002) 123.
3 S. W. S. McKeever: Radiat. Prot. Dosim. **109** (2004) 269.
4 C. W. E. van Eijk: Nucl. Instrum. Methods Phys. Res., Sect. A **460** (2001) 1.
5 T. Kato, G. Okada, and T. Yanagida: Radiat. Meas. **92** (2016) 93.
6 G. Okada, Y. Koguchi, T. Yanagida, S. Kasap, and H. Nanto: Jpn. J. Appl. Phys. **62** (2023) 010609.
7 P. Lecoq: Nucl. Instrum. Methods Phys. Res. A: Accel. Spectrom. Detect. Assoc. Equip. **809** (2016) 130.
8 H. Kimura, T. Kato, T. Fujiwara, M. Tanaka, D. Nakauchi, N. Kawaguchi, and T. Yanagida: Jpn. J. Appl. Phys. **62** (2023) 010504.
9 T. Yanagida, Y. Fujimoto, T. Ito, K. Uchiyama, and K. Mori: Appl. Phys. Express **7** (2014) 062401.
10 T. Kato, D. Nakauchi, N. Kawaguchi, and T. Yanagida: Jpn. J. Appl. Phys. **62** (2023) 010604.
11 E. G. Yukihara and T. Kron: Radiat. Prot. Dosimetry **192** (2020) 122.
12 Y. Endo, K. Ichiba, D. Nakauchi, T. Kato, N. Kawaguchi, and T. Yanagida: Sens. Mater. **36** (2024) 473.
13 K. Okazaki, D. Nakauchi, H. Fukushima, T. Kato, N. Kawaguchi, and T. Yanagida: Sens. Mater. **35** (2023) 459.
14 K. Yamabayashi, K. Okazaki, D. Nakauchi, T. Kato, N. Kawaguchi, T. Yanagida: Sens. Mater. **36** (2024) 523.
15 T. Suto, N. Kawano, K. Okazaki, Y. Takebuchi, D. Shiratori, H. Fukushima, T. Kato, D. Nakauchi, and T. Yanagida: Radiat. Phys. Chem. **209** (2023) 110981.
16 K. Okazaki, D. Nakauchi, N. Kawano, T. Kato, N. Kawaguchi, and T. Yanagida: Radiat. Phys. Chem. **202** (2023) 110514.
17 M. Koshimizu: Jpn. J. Appl. Phys. **62** (2023) 010503.
18 A. Watanabe, A. Magi, A. Yoko, G. Seong, T. Tomai, T. Adschiri, Y. Hayashi, M. Koshimizu, Y. Fujimoto, and K. Asai: Nanomaterials **11** (2021) 1124.
19 K. Okazaki, D. Nakauchi, A. Nishikawa, T. Kato, N. Kawaguchi, and T. Yanagida: Sens. Mater. **36** (2024) 587.
20 Y. Morishita, K. Hoshi, and T. Torii: Nucl. Instrum. Methods Phys. Res. A: Accel. Spectrom. Detect. Assoc. Equip. **966** (2020) 163795.
21 Z. Wu, J. Cheng, M. Xu, B. Wang, Q. Wang, A. Yu, Y. Zhang, W. Wen, and Y. Wu: Appl. Radiat. Isot. **199** (2023) 110867.
22 T. Kunikata, T. Kato, D. Shiratori, D. Nakauchi, N. Kawaguchi, and T. Yanagida: Jpn. J. Appl. Phys. **61** (2022) 062008.
23 S. Toyama, M. Daiki, M. Miwa, and S. Matsuyama: Radiat. Meas. **169** (2023) 107027.
24 S. A. McElhaney, J. A. Ramsey, M. L. Bauer, and M. M. Chiles: Nucl. Instrum. Methods Phys. Res., Sect. A **299** (1990) 111.
25 Y. Morishita, S. Yamamoto, K. Izaki, J. H. Kaneko, K. Toui, Y. Tsubota, and M. Higuchi: Nucl. Instrum. Methods Phys. Res., Sect. A **764** (2014) 383.

26 Y. Takebuchi, M. Koshimizu, K. Ichiba, T. Kato, D. Nakauchi, N. Kawaguchi, and T. Yanagida: Materials **16** (2023) 4502.
27 Q. Shi, Y. Huang, K. V. Ivanovskikh, V.A. Pustovarov, L. Wang, C. Cui, and P. Huang: J. Alloys Compd. **817** (2020) 152704.
28 T. Yanagida, K. Kamada, Y. Fujimoto, H. Yagi, and T. Yanagitani: Opt. Mater. **35** (2013) 2480.
29 B. Yang, Z. Yang, Y. Liu, F. Lu, P. Li, Y. Yang, and X. Li: Ceram. Int. **38** (2012) 4895.
30 A. N. Trukhin, K. Shmits, J. L. Jansons, and L. A. Boatner: J. Phys. Condens. Matter. **25** (2013) 385502.
31 H. Liang, Y. Tao, Q. Su, and S. Wang: J. Solid State Chem. **167** (2002) 435.
32 X. Wu, H. You, H. Cui, X. Zeng, G. Hong, C. H. Kim, C. H. Pyun, B. Y. Yu, and C. H. Park: Mater. Res. Bull. **37** (2002) 1531.
33 G. M. Onyshchenko, L. L. Nagornaya, V. G. Bondar, Y. Borodenko, O. V. Zelenskaya, E. N. Pirogov, and V. D. Ryzhikov: Nucl. Instrum. Methods Phys. Res., Sect. A **537** (2005) 394.
34 H. Ezawa, Y. Takebuchi, K. Okazaki, T. Kato, D. Nakauchi, N. Kawaguchi, and T. Yanagida: Sens. Mater. **36** (2024) 465.
35 H. Ezawa, K. Okazaki, Y. Takebuchi, T. Kato, D. Nakauchi, N. Kawaguchi, and T. Yanagida: Solid State Sci. **157** (2024) 107715.
36 T. Yanagida: J. Lumin. **169** (2016) 544.
37 D. Totsuka, T. Yanagida, Y. Fujimoto, Y. Yokota, F. Moretti, A. Vedda, and A. Yoshikawa: Appl. Phys. Express. **5** (2012) 052601.
38 K. Miyazaki, D. Nakauchi, T. Kato, N. Kawaguchi, and T. Yanagida: J. Mater. Sci. Mater. Electron. **34** (2023) 1082.
39 D. J. Robbins: J. Electrochem. Soc. **127** (1980) 2694.
40 J. Lin, Y. Hu, L. Chen, Z. Wang, and S. Zhang: Phys. Rev. B Condens. Matter. **485** (2016) 39.
41 J. Wang, J. Wang, and P. Duan: Mater. Lett. **107** (2013) 96.